Available online at www.sciencedirect.com

SCIENCE @ DIRECT®

Polymer 45 (2004) 2081–2091

polymer

www.elsevier.com/locate/polymer

Polymer Communication

Effects of organic nucleating agents and zinc oxide nanoparticles on isotactic polypropylene crystallization

Jianguo Tang[a,b], Yao Wang[a], Haiyan Liu[a], Laurence A. Belfiore[b,*]

[a]*College of Chemical Engineering, Qingdao University, Qingdao 266071, People's Republic of China*
[b]*Polymer Physics and Engineering Laboratory, Department of Chemical Engineering, Colorado State University, Fort Collins, CO 80523, USA*

Received 15 April 2003; received in revised form 3 November 2003; accepted 12 November 2003

Abstract

Organic nucleating agents and inorganic nanoparticles, as well as their hybrid composites, affect the crystallization temperature and morphology of the monoclinic α-form of isotactic polypropylene (iPP). Techniques such as differential scanning calorimetry, hot-stage optical microscopy with cross polars, wide angle X-ray diffraction, and transmission electron microscopy were employed. Nanoparticles of zinc oxide function as efficient supports for 1,3,5-benzene tricarboxylic-(*N*-2-methylcyclohexyl)triamine because the temperature at which the maximum rate of iPP crystallization occurs during 10 °C/min cooling from the molten state increases from 111 °C for the pure polymer to 125 °C at low concentrations of this hybrid nucleating agent. In the absence of zinc oxide, 0.06 wt% of this aliphatic triamine recrystallizes near 165 °C and increases the crystallization temperature of iPP by 7 °C, relative to the pure polymer. Fluorinated aromatic triamines, such as 1,3,5-benzene tricaboxylic-(*N*-4-fluorophenyl)triamine, are weak nucleating agents that reduce spherulite size in isotactic polypropylene but only increase the crystallization temperature marginally when the polymer is cooled from the molten state. Both micro- and nanoparticles of zinc oxide reduce spherulite size in isotactic polypropylene, but smaller spherulites are observed when the inorganic nanoparticles exhibit dimensions on the order of 40–150 nm relative to micron-size particles. In contrast, 0.06 wt% of the aliphatic triamine in iPP yields a distorted birefringent texture under cross polars that is not spherulitic. Non-spherulitic birefringent textures in iPP are also observed when the aliphatic triamine nucleating agent is coated onto micro- or nanoparticles of zinc oxide. This study demonstrates that the nonisothermal crystallization temperature of isotactic polypropylene increases by an additional 7 °C when an aliphatic triamine is distributed efficiently within the polymeric matrix by coating this nucleating agent onto zinc oxide nanoparticles.

Keywords: Isotactic polypropylene; Zinc oxide nanoparticles; Organic triamine nucleating agents

---

1. Introduction

Nucleation mechanisms for semicrystalline polymers have a significant influence on the morphology of the crystalline phase. The number and size distribution of nucleation sites affect product performance. In many cases, when there is a deliberate attempt to control polymer properties by manipulating morphology, nucleating agents are used. There are a few hundred publications in the research literature that focus on polymer crystallization via organic [1] and inorganic [2] nucleating agents. However, there are only 10–15 investigations based on nanoscale-size nucleating agents for polymers, in general, and even fewer that employ nanoparticles of zinc oxide [3]. The most common polymers whose crystallization kinetics have been enhanced by nucleating agents are (i) isotactic polypropylene (iPP), (ii) poly(ethylene terephthalate) (PET), and (iii) nylon 6. Several hundred publications discuss nucleation in polypropylene, but there are more than an order-of-magnitude fewer that employ inorganic nucleating agents. The use of inorganic nanoparticle nucleating agents for iPP is extremely rare [4,5]. Zhang et al. [5] studied the mechanical properties and crystallization behaviour of isotactic polypropylene composites with crosslinked styrene-butadiene nanoparticles that contain sodium benzoate. The stiffness of these nanocomposites is enhanced because the nucleation density is higher and the crystallization kinetics of iPP proceed faster in the presence of ultrafine elastomeric particles with length scales below 100 nm [5]. Gui et al. [6] report that 0.8 wt% of an organic phosphorus nucleating agent dispersed in iPP increases the calculated

---

[*] Corresponding author. Tel.: +1-970-491-5395; fax: +1-970-491-7369.
E-mail address: belfiore@engr.colostate.edu (L.A. Belfiore).

0032-3861/$ - see front matter © 2003 Elsevier Ltd. All rights reserved.
doi:10.1016/j.polymer.2003.11.046

nucleation density by six orders of magnitude, and the crystallization temperature is enhanced by 12 °C. Hydrophobic nano-silicates with good wettability and dispersion characteristics enhance thermal stability, reinforce mechanical properties and increase the crystallization temperature of poly(ethylene terephthalate) [7]. However, hydrophilic nano-silicates in PET, which also increase its crystallization temperature, induce shear-thinning behaviour at very low frequencies in dynamic rheometry and function as viscosity-reducers [7]. There do not seem to be any references in the ISI Web of Science™ database where inorganic nanoparticles are employed as nucleating agents for polyamides.

Nucleating agents can be classified as natural [8] or synthetic [9]. In most cases, dibenzylidene sorbitol and 3,4-dimethyldibenzylidene sorbitol, at concentrations between 0.5 and 1.5 wt%, increase the rate of polymer crystallization and the temperature at which the maximum rate of crystallization occurs upon cooling from the molten state [9]. Organocarboxylic acids function as nucleating agents for polyolefins because their polar groups make them insoluble in the molten polymer, and their organic groups provide the necessary wetting characteristics that are required when a foreign surface is implanted in the molten polymer. Molecular interactions between the polymer and the surface of the nucleating agent must be operative to increase the rate of crystallization and the temperature at which the maximum rate occurs upon cooling from the molten state [10–12]. These polymer-surface interactions reduce the interfacial free energy barrier for spontaneous nucleation and growth of a birefringent dendritic phase in the molten polymer. When the nucleation induction period is shorter and the number of primary nucleation sites increases, the overall rate of crystallization increases. Heterogeneous nucleating agents have been used industrially to reduce process cycle times, induce crystallization at smaller degrees of supercooling (i.e. $T_{\mathrm{melt}} - T_{\mathrm{crystallization}}$), and produce translucent materials with smaller crystallite sizes [13].

Several classes of inorganic compounds can be employed as nucleating agents [14,15], but the oxides of aluminum (Al_2O_3), calcium (CaO), silicon (SiO_2), titanium (TiO_2), and zinc (ZnO) are most useful. Recent developments in nanotechnology [16] have provided several routes to nanoscale-sized particles of metal oxides. In this research contribution, a unique deposition method is employed to prepare nanoparticles of zinc oxide [16]. Both micro- and nanoscale-size zinc oxides function as inorganic supports for organic nucleating agents.

Typical organic nucleating agents for semicrystalline polymers are based on the modification of sorbitol [9, 17–21]. Shepard et al. [17] found that dibenzylidene sorbitol (DBS) undergoes self-assembly and promotes the formation of spherulites in commercially important polyolefins, such as polypropylene. Isothermal and nonisothermal crystallization kinetics of virgin and DBS-nucleated isotactic polypropylene were investigated by Feng et al. [18]. The primary objectives of this investigation were to; (i) compare the crystallization temperatures of isotactic polypropylene upon cooling from the molten state in the presence of organic nucleating agents and zinc oxide nanoparticles, and (ii) correlate nucleation efficiencies, based on an increase in the temperature (i.e. T_C) at which the maximum rate of nonisothermal crystallization occurs, with the solid state morphology of this industrially important polyolefin.

2. Experimental considerations

2.1. Materials

Isotactic polypropylene (iPP) was purchased from Elf-AtoChem (Paris, France) with a number-average molecular weight of 3×10^5 Da and a polydispersity of 5.5. It was pulverized cryogenically in a micro-mill prior to investigation. Micron-size zinc oxide (i.e. MicroZn), with length scales on the order of 1 μm, was obtained from Tai Xing Nano-Materials, Jiangshu, China. Nanoparticles of zinc oxide (i.e. NanoZn) were synthesized using the procedure described in reference [16]. Aqueous solutions of zinc acetate and urea, at a Zn^{2+}/urea molar ratio of 1:9, were mixed with vigorous agitation and ultrasonic vibration. Reactions (1) and (2) were carried out at 95 ± 2 °C for 2–2.5 h.

$$CO(NH_2)_2 + 3H_2O \Rightarrow CO_2 + 2NH_3{\cdot}H_2O \quad (1)$$

$$Zn(OOCCH_3)_2 + 2NH_3{\cdot}H_2O \Rightarrow Zn(OH)_2 + 2CH_3COO^- + 2NH_4^+ \quad (2)$$

The third reaction which produces zinc oxide occurred between 220 and 450 °C;

$$Zn(OH)_2 \Rightarrow ZnO + H_2O \quad (3)$$

The products were (i) washed twice in distilled water with vigorous agitation and ultrasonic vibration for 20 min, and (ii) filtered under vacuum. Two more washing cycles were performed in ethanol. Dried nanoparticles of zinc oxide exhibit dimensions on the order of 30–40 nm. Organic nucleating agents, 1,3,5-benzene tricarboxylic-(*N*-2-methylcyclohexyl)triamine (i.e. $OrganoCH_3$) and 1,3,5-benzene tricaboxylic-(*N*-4-fluorophenyl)triamine (i.e. OrganoF) were synthesized via the catalytic reactions of 1,3,5-benzene tricarboxylic chloride and amine derivatives (i.e. RNH_2), where the functional group R was 2-methylcyclohexylamine to produce $OrganoCH_3$, and 4-fluoroaniline for OrganoF. All reagents were obtained from Aldrich Chemical Company in Milwaukee, Wisconsin.

2.2. Sample preparation

Inorganic particles (MicroZn or NanoZn) and cryogenically pulverized isotactic polypropylene were mixed as solid powders at ambient temperature via rotation in a cylindrical vial at 30 rpm for 48 h. The same procedure was employed to prepare samples of pure iPP and mixtures of iPP with zinc oxide. Needle-like crystals of OrganoCH$_3$ or OrganoF were ground into fine powders and mixed with iPP via the same procedure. Hybrid organic–inorganic composites were prepared as follows. OrganoCH$_3$ or OrganoF was dissolved in dimethylformamide (DMF) at 120 °C for 3 h. Then, zinc oxide particles were added to this solution under stirring. Gradual controlled cooling to ambient temperature allowed OrganoCH$_3$ or OrganoF to recrystallize on the zinc oxide particles. In some cases, it was necessary to add ethylene glycol to the DMF suspension of the organic nucleating agent and zinc oxide below 30 °C, which allowed either OrganoCH$_3$ or OrganoF to precipitate onto the surface of the zinc oxide particles. These micro and nanoscale-size coated particles were mixed with cryogenically pulverized isotactic polypropylene at ambient temperature via rotation in a cylindrical vial at 30 rpm for 48 h. Since isotactic polypropylene degrades initially at 225 °C in an oxygen atmosphere [22], homogeneous solid samples of iPP with the appropriate nucleating agent were prepared in a high-shear twin-screw micro-mixer with recycle (DSM Research, The Netherlands) under a nitrogen blanket at 239 °C. The screw speed was 45 rpm, the mixing time in the extruder was 4 min for each 4-gram sample, and 3–4 min were required to recover each 4-gram extrudate at ambient temperature. The initial 8 grams of extrudate in the first two batches were discarded, before samples were collected and analyzed.

2.3. Thermal analysis

A Perkin–Elmer DSC-7 was used for calorimetric investigations of nonisothermal crystallization. Calibration was performed using pure indium at a heating rate of 10 °C/min. Each sample of iPP was heated from 50 °C to 230 °C at a rate of 10 °C/min, soaked isothermally at 230 °C for 5 min to allow complete melting of the polymer, and then cooled to 50 °C at 10 °C/min. Each sample of iPP was subjected to two heating/cooling cycles under a dry nitrogen purge, and data were recorded during the second cooling.

2.4. Polarized optical microscopy

Birefringent patterns were detected using a Nikon Diaphot 300 optical microscope with cross polars and a Mettler FP80 heated stage. Extruded samples were placed between two microscope slides, heated from ambient to 275 °C at a rate of 10 °C/min, soaked at 275 °C for 5 min to ensure complete melting of OrganoCH$_3$ or OrganoF, and cooled to ambient at 10 °C/min. A dry nitrogen purge was employed for all high-temperature experiments.

2.5. Wide-angle X-ray diffraction

All measurements were obtained at ambient temperature on a Huber/Seifert Iso-Debyeflex 3003 (Bruker AXS) X-ray diffractometer using Cu Kα radiation. Samples for wide-angle X-ray diffraction were injection molded under a nitrogen blanket at 260 °C and transferred at ambient temperature to a circular mold with a diameter of 20 mm and a thickness of 1 mm.

2.6. Transmission electron microscopy

Micrographs were obtained from a Zeiss 902 transmission electron microscope at ambient temperature. Polypropylene samples containing MicroZn or NanoZn were freeze-fractured in liquid nitrogen and microtomed directly without OsO$_4$ staining.

3. Results and discussion

3.1. Influence of zinc oxide nanoparticles on the morphology and crystallization temperature of isotactic polypropylene

At a cooling rate of 10 °C/min in the calorimeter, the maximum rate of crystallization occurs at 111 °C for pure isotactic polypropylene, as illustrated by the lowermost thermogram of Fig. 1. This crystallization temperature agrees with the one measured by Marcos et al. [22] at the same cooling rate for a completely melted sample of polypropylene that is 95% isotactic with a viscosity-average molecular weight of 1.64×10^5 Da. The other thermograms

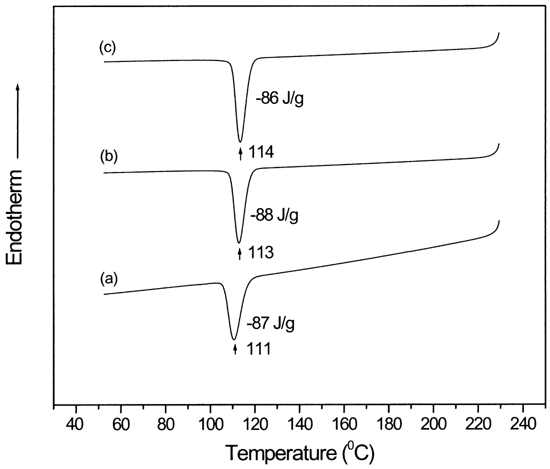

Fig. 1. DSC cooling traces for (a) isotactic polypropylene, (b) iPP with 2 wt% micron-size particles of zinc oxide (i.e. MicroZn), and (c) iPP with 2 wt% nanoparticles of zinc oxide (i.e. NanoZn). The cooling rate was 10 °C/min. All samples were extruded at 239 °C from a twin-screw micro-mixer.

in Fig. 1 reveal that this crystallization temperature increases marginally by 2 or 3 °C in the presence of 2 wt% MicroZn (i.e. $T_C = 113$ °C) or NanoZn (i.e. $T_C = 114$ °C). Wide-angle X-ray diffraction measurements in Fig. 2 reveal that pure iPP and its mixtures with 2 wt% MicroZn or NanoZn crystallize primarily in the monoclinic α-form via reflections at $2\Theta = 14.1$, 16.8, 18.6 and 21.8 degrees [23,24]. The diffractograms in Fig. 2 indicate that the crystal structure of the α-form of isotactic polypropylene is essentially unaffected by zinc oxide. These observations are consistent with other studies of polypropylene composites filled with inorganic nanoparticles [4]. However, Privalko et al. [4] identified a small-angle X-ray scattering reflection in iPP that was absent in the inorganic-filled polymeric nanocomposites. All three diffractograms in Fig. 2 also indicate the presence of the β-form of iPP via reflections at $2\Theta = 16.1$ and 21.1° [23,24]. Organic anthraquinone pigments [25], *N*,*N*-dicyclohexyl-2,6-naphthalenedicarboxamide [23], and dicyclohexylterephthalamide [32] nucleate the hexagonal β-form of isotactic polypropylene. Optical micrographs viewed with cross polars of the same three iPP samples in Fig. 3 were obtained at 105 °C after cooling from the molten state. The largest spherulitic dimensions on the order of 150–200 μm are observed for pure iPP in Fig. 3(a), (left). Much smaller spherulitic dimensions appear in iPP samples that contain either MicroZn [Fig. 3(b), middle, ≈50 μm diameter] or NanoZn [Fig. 3(c), right, ≈25 μm diameter]. Nanoparticles of zinc oxide produce the smallest iPP spherulites in Fig. 3(c), with dimensions on the order of 25 μm. These results are consistent with those reported by Wu and Xu [26], where nanoparticles of SiO_2 increase the crystallization temperature of iPP by 3–4 °C and reduce spherulite size. Marco et al. [22] observed an increase in the nucleation density (i.e. 71% efficiency), an increase in the degree of crystallinity from 52% for the undiluted polymer to 62% at a cooling rate of 1 °C/min., and a birefringent but non-spherulitic texture when the monoclinic phase (i.e. α-form) of isotactic polypropylene was nucleated by 0.05 wt.% of an organic phosphate derivative. Unstained TEM micrographs (i.e. negatives) in Fig. 4 identify length scales for the zinc oxide particles in iPP. Micron-size particles are rectangular with a linear dimension of about 1 μm [Fig. 4(a), left]. Individual nanoscale-size particles are approximately 40 nm, whereas agglomerated nanoparticles are 150 nm in length [Fig. 4(b), right]. The nano-zinc-oxide particles (i.e. NanoZn) in Fig. 4(b) exhibit better dispersion and larger specific surface area relative to MicroZn in Fig. 4(a). Gutzow et al. [27,28] developed a theory to explain why inorganic particles nucleate crystallization in linear polyolefins. Nucleation efficiencies are related to (i) bond energies between the nucleating agent and the polymeric crystals, and (ii) crystallographic mismatches between substrate and polymer.

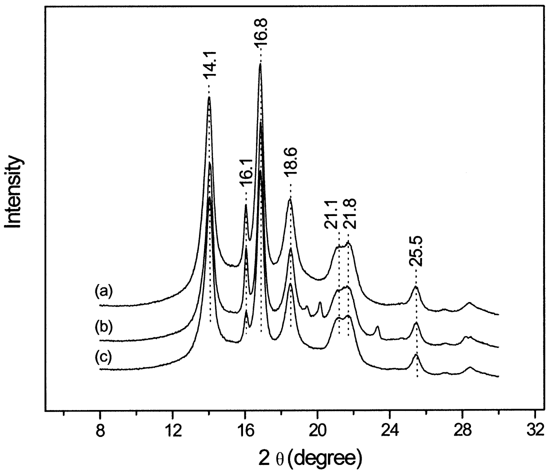

Fig. 2. Ambient temperature X-ray diffractograms for (a) isotactic polypropylene, (b) iPP with 2 wt% micron-size particles of zinc oxide (i.e. MicroZn), and (c) iPP with 2 wt% nanoparticles of zinc oxide (i.e. NanoZn). All samples were injection molded at 260 °C. The monoclinic α-form of iPP yields reflections at the following Bragg scattering angles (i.e. 2Θ) and corresponding Miller indices; 14.1° (110), 16.8° (040), 18.6° (130), 21.1° (111), 21.8° (131) and (041). The hexagonal β-form of iPP exhibits the following reflections [23,24] and corresponding Miller indicies; $2\Theta =$ 16.1° (300) and 21.1° (301). Weak diffraction peaks at $2\Theta = 19.5°$, 20.2° and 23.4° in diffractogram (b) could be due to a separate phase of micron-size particles of zinc oxide [37].

3.2. Organic nucleating agents for isotactic polypropylene

Previous investigations of organic nucleating agents with different efficiencies for inducing iPP crystallization have included (i) natural compounds and their derivatives [9,18], like dibenzylidene sorbitol, (ii) organic salts such as sodium benzoate [14,29], (iii) organic phosphate salts [30], and (iv) low-molecular-weight polymers, like poly(α-pinene) [31]. Sodium benzoate increases the crystallization temperature of iPP by 15 °C and decreases the isothermal and nonisothermal crystallization half-times at concentrations that approach its equilibrium solubility in the molten polymer [14,29]. Hence, sodium benzoate functions as a good nucleating agent for the α-form of iPP. Thermograms in Fig. 5 reveal the effectiveness of OrganoCH$_3$ as a nucleating agent for iPP. Mixtures of iPP and 0.06 wt% OrganoCH$_3$ exhibit a crystallization temperature of 118 °C in thermogram (b) of Fig. 5 at a cooling rate of 10 °C/min. Hence OrganoCH$_3$ increases the crystallization temperature of iPP by 7 °C, whereas both MicroZn and NanoZn have negligible effects on T_C, as illustrated in Fig. 1. Crystallization exotherms for iPP and 0.06 wt% OrganoF are presented in Fig. 6. This fluorinated aromatic compound decreases spherulite size, but it has an insignificant effect on the crystallization temperature of iPP. Optical micrographs viewed with cross polars at 200 × magnification in Fig. 7(a) (left) reveal that iPP crystallites are birefringent but not spherulitic, when nucleation is induced by OrganoCH$_3$. Crystallites of the monoclinic α-form of iPP do not evolve in spherically symmetric fashion from their inception [33–36]. Instead, spherulitic superstructures develop from

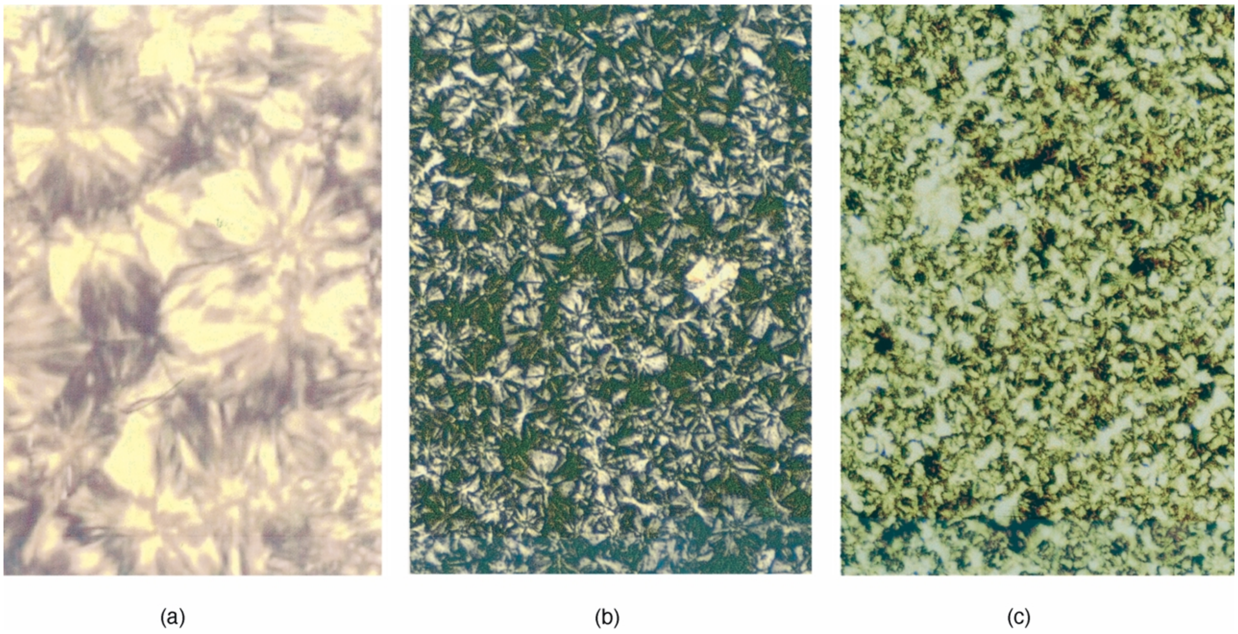

Fig. 3. Optical micrographs viewed with cross polars at 200 × magnification (i.e. 1 cm = 60 μm) for (a) isotactic polypropylene, (b) iPP with 2 wt% micron-size particles of zinc oxide (i.e. MicroZn), and (c) iPP with 2 wt% nanoparticles of zinc oxide (i.e. NanoZn). Samples were extruded at 239 °C from a twin-screw micro-mixer, and all photos were obtained at 105 °C. There is a significant decrease in spherulite dimensions when micron-size and nanoparticles of zinc oxide are present.

much simpler dendritic chain-folded crystal precursors [33]. Hence, the absence of spherulites in Fig. 7(a) does not imply that OrganoCH$_3$ induces a mode of crystallization that is fundamentally different from the process in pure iPP. When these dendritic precursors form in OrganoCH$_3$-nucleated iPP, impingement might occur during the early stages of growth before the dendrites develop completely into spherulites. In contrast, the presence of OrganoF yields fairly well-defined iPP spherulites in Fig. 7(b) (right) that are larger than iPP spherulites in the presence of MicroZn in Fig. 3(b), but smaller than those for pure iPP in Fig. 3(a).

Coherent Bragg scattering peaks in the diffractograms of

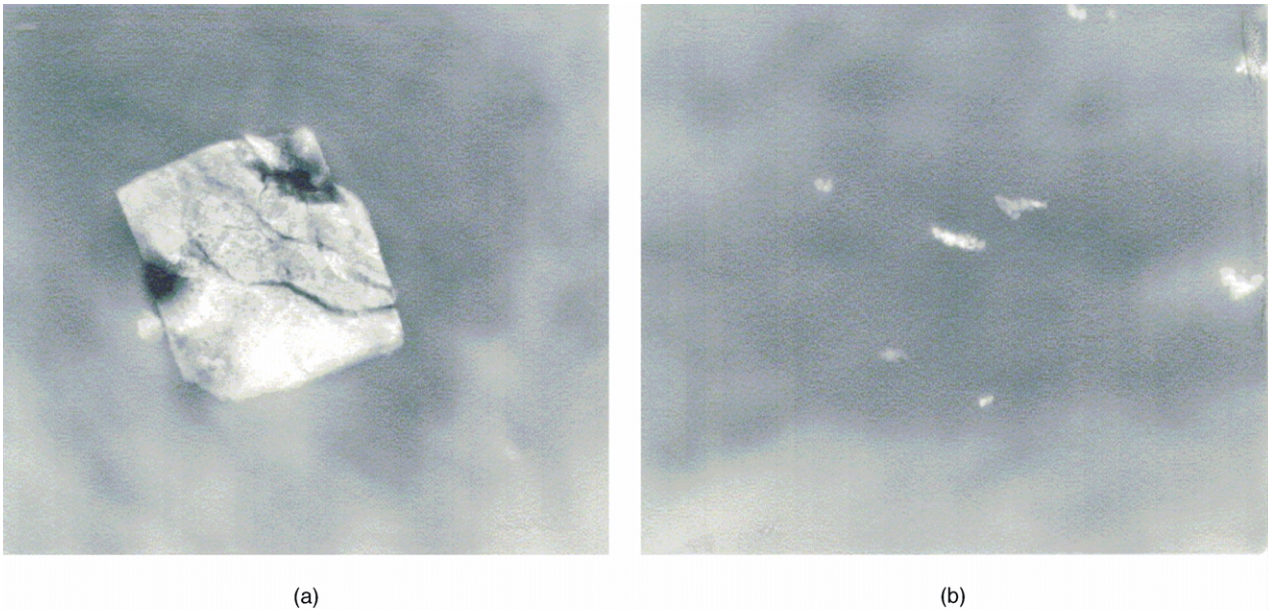

Fig. 4. Ambient temperature unstained TEM images (i.e. negatives) of (a) iPP containing 2 wt% micron-size particles of zinc oxide (i.e. MicroZn), 1 cm ≈ 0.44 μm which corresponds to a magnification of ≈23,000 ×, and (b) iPP containing 2 wt% nanoparticles of zinc oxide (i.e. NanoZn), 1 cm ≈ 0.29 μm which corresponds to a magnification of ≈35,000 ×. The surface of the micron-size zinc oxide particles in (a) is smooth and their shape is rectangular. Separate nanoparticles of zinc oxide in (b) have dimensions of approximately 40 nm, whereas the agglomerated particles have lengths of about 150 nm. All samples were extruded at 239 °C from a twin-screw micro-mixer.

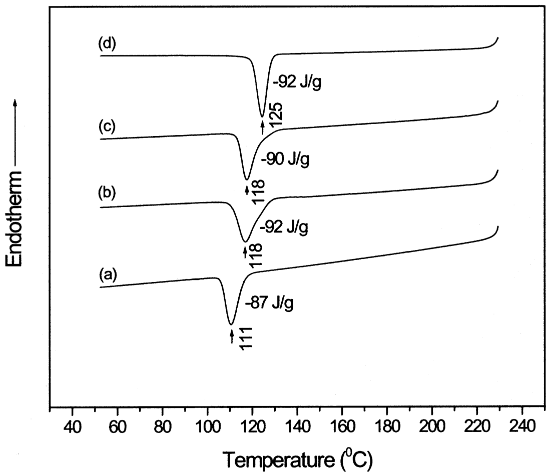

Fig. 5. DSC cooling traces of (a) isotactic polypropylene, (b) iPP nucleated by 0.06 wt% OrganoCH_3, (c) iPP nucleated by 0.3 wt% micron-size particles of zinc oxide (i.e. MicroZn) that were coated with 0.06 wt% OrganoCH_3, and (d) iPP nucleated by 0.3 wt% nanoparticles of zinc oxide (i.e. NanoZn) that were coated with 0.06 wt% OrganoCH_3. The cooling rate was 10 °C/min. All samples were extruded at 239 °C from a twin-screw micro-mixer. The maximum nonisothermal crystallization temperature of iPP (i.e. 125 °C) occurs when NanoZn is coated with OrganoCH_3 in thermogram (d).

Figs. 8 and 9 reveal that both OrganoCH_3 and OrganoF primarily induce crystallization of the α-form of iPP, because the strongest reflections in Figs. 2, 8 and 9 appear at the same scattering angles. A comparison of the crystallographic reflections at scattering angles of 16.1 and 16.8° in diffractograms (a) and (b) of Figs. 8 and 9 suggests that OrganoCH_3 induces a larger fraction of iPP to crystallize in the β-form, relative to OrganoF. This enhancement of the β-form of iPP by OrganoCH_3 is verified by the relative intensities of the reflections at 21.1° (i.e. β-form [23,24]) and 21.8° (i.e. α-form) in diffractograms (a) and (b) of Fig. 8. There is no difference in the relative intensities of these reflections for all of the diffractograms in Fig. 9, when OrganoF is present in isotactic polypropylene. OrganoCH_3 not only increases the crystallization temperature of iPP more than OrganoF [i.e. 7 °C vs. 2 °C via thermograms (a) and (b) of Figs. 5 and 6], but coherent reflections at scattering angles of 14.1 and 16.8° in diffractograms (a) and (b) of Figs. 8 and 9 suggest that there is a slightly higher degree of iPP crystallinity, relative to (i) the pure polymer and (ii) iPP with OrganoF, when nucleation occurs via OrganoCH_3. However, this trend is verified only marginally by the enthalpy of crystallization in thermograms (a) and (b) of Figs. 5 and 6. In summary, OrganoCH_3 increases the crystallization temperature of iPP by 7 °C, induces a larger fraction of the polymer to crystallize in the β-form, and seems to increase the overall weight fraction of crystallinity, while the spherulitic superstructure is disrupted significantly. OrganoF increases T_C of iPP by 2 °C, does not affect the fraction of the polymer that crystallizes in the β-form, marginally increases the overall weight fraction of crystallinity, and retains the spherulitic superstructure of iPP, even though spherulite size is reduced relative to pure iPP.

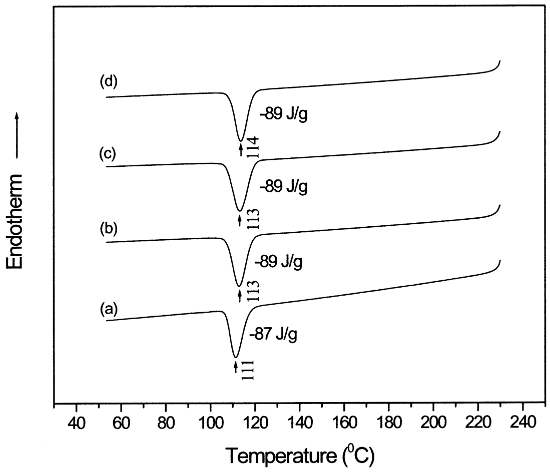

Fig. 6. DSC cooling traces of (a) isotactic polypropylene, (b) iPP containing 0.06 wt% OrganoF, (c) iPP containing 0.3 wt% micron-size particles of zinc oxide (i.e. MicroZn) that were coated with 0.06 wt% OrganoF, and (d) iPP containing 0.3 wt% nanoparticles of zinc oxide (i.e. NanoZn) that were coated with 0.06 wt% OrganoF. The cooling rate was 10 °C/min. All samples were extruded at 239 °C from a twin-screw micro-mixer.

Optical micrographs in Fig. 10 depict morphological developments when the polarizer and analyzer are perpendicular to each other. These data shed light on the evolution of isotactic polypropylene crystallization induced by the organic nucleating agent, OrganoCH_3. Micrographs were recorded at (a) 200 °C and (b) 285 °C during heating, and (c) 165 °C and (d) 129 °C during the cooling trace. These samples were prepared differently from the extrudates discussed previously. Needle-like crystals of OrganoCH_3 were not ground into fine powders. Instead, they were spread on glass slides and covered with cryogenically pulverized isotactic polypropylene. Hence, the organic nucleating agent was observed using cross-polarized light as the needle-like crystals melted and recrystallized within an isotropic polymer matrix. Heating and cooling profiles within the temperature-controlled stage were implemented under a dry nitrogen blanket to monitor the morphological state of the nucleating agent within the polymer matrix, as well as recrystallization of both components during the cooling trace. Isotactic polypropylene melts at 165 °C. Needle-like birefringent structures of OrganoCH_3 were observed at 200 °C in Fig. 10(a) because the polymer is isotropic at this temperature. At 285 °C, OrganoCH_3 is completely melted and dissolved in the molten polymer, and the isotropic nature of these mixtures is verified by nonbirefringent darkness in Fig. 10(b). Upon cooling from the molten state, birefringent needles of OrganoCH_3 appear at 165 °C in Fig. 10(c), as recrystallization of the organic nucleating agent occurs in molten iPP. These birefringent needles in Fig. 10(c), which are smaller than their counterparts in Fig. 10(a), function as nucleation sites for

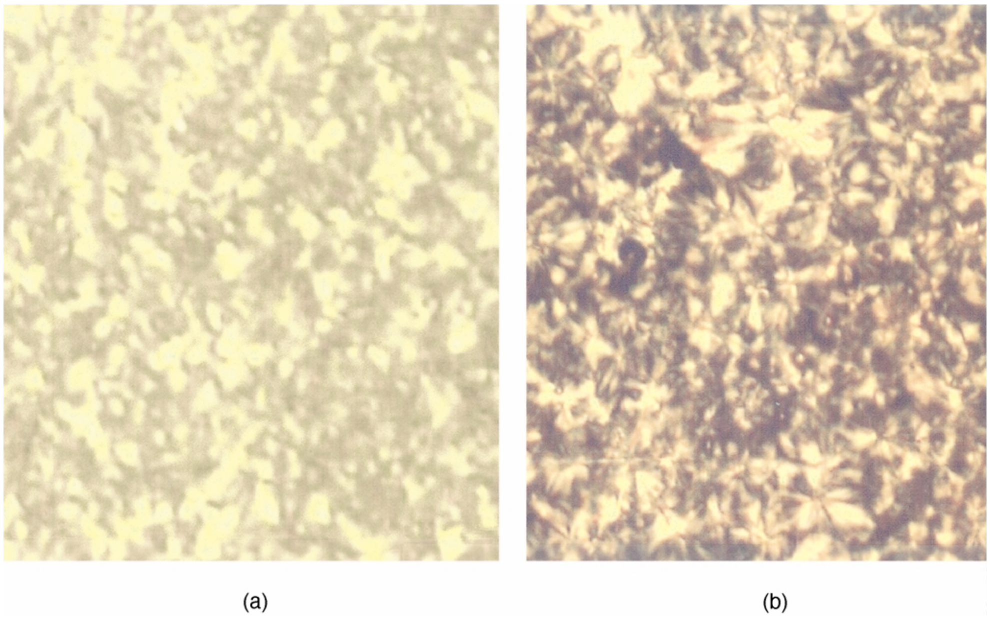

Fig. 7. Optical micrographs viewed with cross polars at 200 × magnification (i.e. 1 cm = 60 μm) for (a) isotactic polypropylene nucleated by 0.06 wt% OrganoCH$_3$, revealing a birefringent, but non-spherulitic, texture, and (b) isotactic polypropylene containing 0.06 wt% OrganoF, which contains space-filling spherulites. Samples were extruded at 239 °C from a twin-screw micro-mixer, and all photos were obtained at 105 °C.

the crystallization of iPP on OrganoCH$_3$ at 129 °C in Fig. 10(d).

3.3. Zinc oxide nanoparticle supports for organic nucleating agents

The data in Fig. 1 indicate that 2 wt% MicroZn and NanoZn have an insignificant effect on the crystallization temperature of isotactic polypropylene. Thermogram (b) in Fig. 6 also reveals that 0.06 wt% OrganoF has an insignificant effect on T_C. The crystallization exotherm at 118 °C in thermogram in Fig. 5(b) supports the claim that OrganoCH$_3$ induces the largest increase in iPP's T_C, based on the additives investigated in this study. If specific surface area is an important factor governing the efficiency of nucleating agents [17], then it should be feasible to use nanoparticles of zinc oxide (i.e. NanoZn) as a dispersed-phase support for OrganoCH$_3$ in the iPP matrix. Relative to pure isotactic polypropylene with $T_C = 111$ °C, OrganoCH$_3$-coated particles of NanoZn increase the crystallization temperature of iPP by 14 °C in thermogram 5(d). Relative to iPP with uncoated particles of NanoZn, in

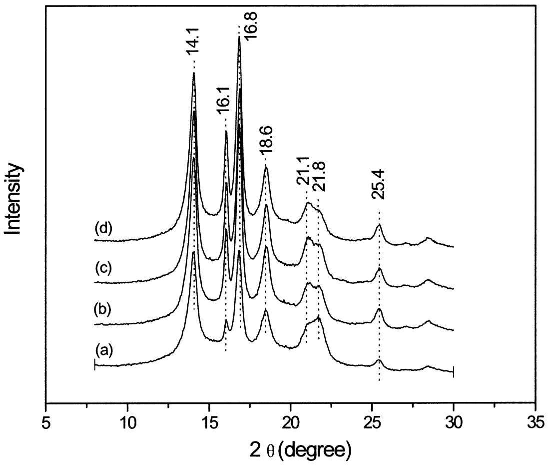

Fig. 8. Ambient temperature X-ray diffractograms for (a) isotactic polypropylene, (b) iPP nucleated by 0.06 wt% OrganoCH$_3$, (c) iPP nucleated by 0.3 wt% micron-size particles of zinc oxide (i.e. MicroZn) that were coated with 0.06 wt% OrganoCH$_3$, and (d) iPP nucleated by 0.3 wt% nanoparticles of zinc oxide (i.e. NanoZn) that were coated with 0.06 wt% OrganoCH$_3$. All samples were injection molded at 260 °C.

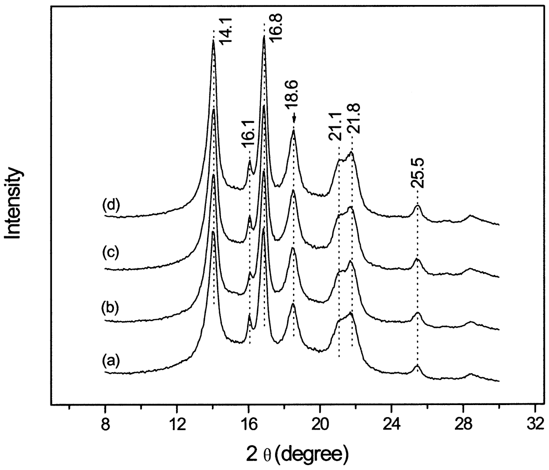

Fig. 9. Ambient temperature X-ray diffractograms for (a) isotactic polypropylene, (b) iPP containing 0.06 wt% OrganoF, (c) iPP containing 0.3 wt% micron-size particles of zinc oxide (i.e. MicroZn) that were coated with 0.06 wt% OrganoF, and (d) iPP containing 0.3 wt% nanoparticles of zinc oxide (i.e. NanoZn) that were coated with 0.06 wt% OrganoF. All samples were injection molded at 260 °C.

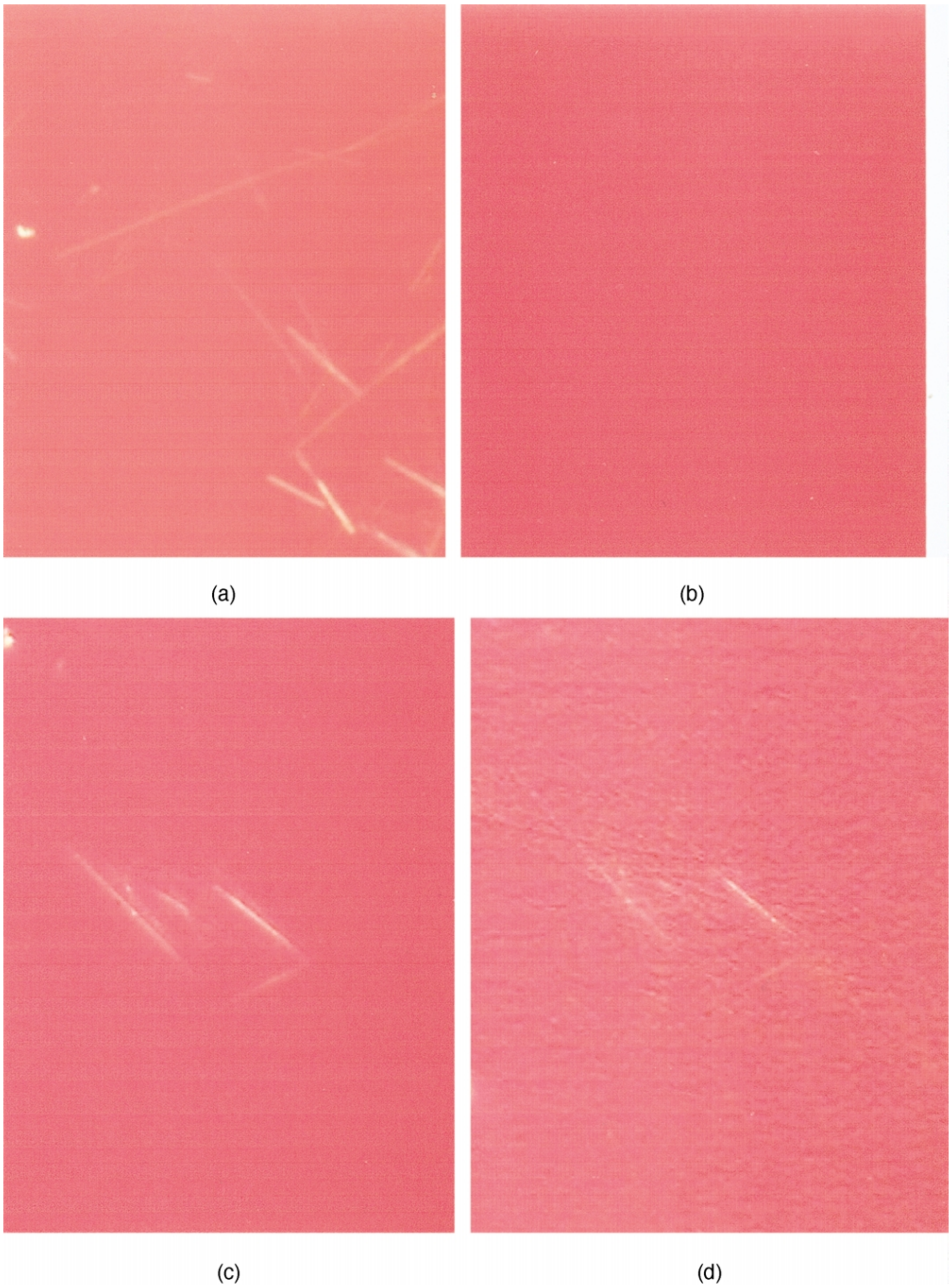
(a) (b) (c) (d)

Fig. 10. Optical micrographs viewed with cross polars and a first-order red retardation plate at 200 × magnification (i.e. 1 cm = 60 μm) for isotactic polypropylene and OrganoCH$_3$ during 10 °C/min heating reveal (a) needle-like crystals of the organic nucleating agent in an isotropic molten polymer matrix at 200 °C, and (b) an isotropic molten mixture at 285 °C. Upon cooling at 10 °C/min, (c) OrganoCH$_3$ recrystallizes at 165 °C in an isotropic molten polymer matrix, and (d) iPP crystallization is nucleated by OrganoCH$_3$ at 129 °C.

which the crystallization temperature of iPP is 114 °C in thermogram 1(c), the OrganoCH$_3$-coated nanoparticles increase T_C by an additional 11 °C even though the organic-coated particle concentration is 6-fold or 7-fold lower than the uncoated nanoparticle concentration in the polymer matrix. Relative to iPP and 0.06 wt% OrganoCH$_3$, in which the crystallization temperature of iPP is 118 °C in thermogram 5(b), the presence of zinc oxide nanoparticles as carriers for the organic nucleating agent causes T_C to increase by an additional 7 °C. The enhancement in T_C is attributed to (i) the effectiveness of OrganoCH$_3$ as a nucleating agent for iPP, (ii) the increase in specific surface area associated with zinc oxide nanoparticles, and (iii) efficient distribution of OrganoCH$_3$ via zinc oxide. One of the most significant increases in the nonisothermal crystallization temperature of the monoclinic form of isotactic polypropylene is 21 °C in the presence of the sodium salt of methylenebis(4,6-di-tert-butylphenyl)phosphate, as reported by Marco et al. [22] at cooling rates between 1 and 10 °C/min. Thermograms in Fig. 5(b) and (c) reveal that the presence of micron-size particles of zinc oxide, coated with OrganoCH$_3$, has no effect on the crystallization temperature of iPP, relative to the nucleation efficiency of the same concentration of OrganoCH$_3$ in iPP without inorganic particles. Furthermore, thermograms in Fig. 6 suggest that the crystallization temperature of iPP in the presence of OrganoF is not affected by coating this fluorinated aromatic compound on zinc oxide nanoparticles in the polymer matrix.

Optical micrographs viewed with cross polars are presented in Fig. 11 for iPP crystallites that have been nucleated by organic-coated zinc oxide micron- and nanoparticles. Similar to Fig. 7(a), OrganoCH$_3$ induces crystallization of iPP without the formation of spherulites in Fig. 11(a) and (b). These non-spherulitic textures are birefringent when OrganoCH$_3$ is coated on either MicroZn [i.e. Fig. 11(a)] or NanoZn [i.e. Fig. 11(b)], and the birefringent dimensions are smaller in Fig. 11(a) and (b)

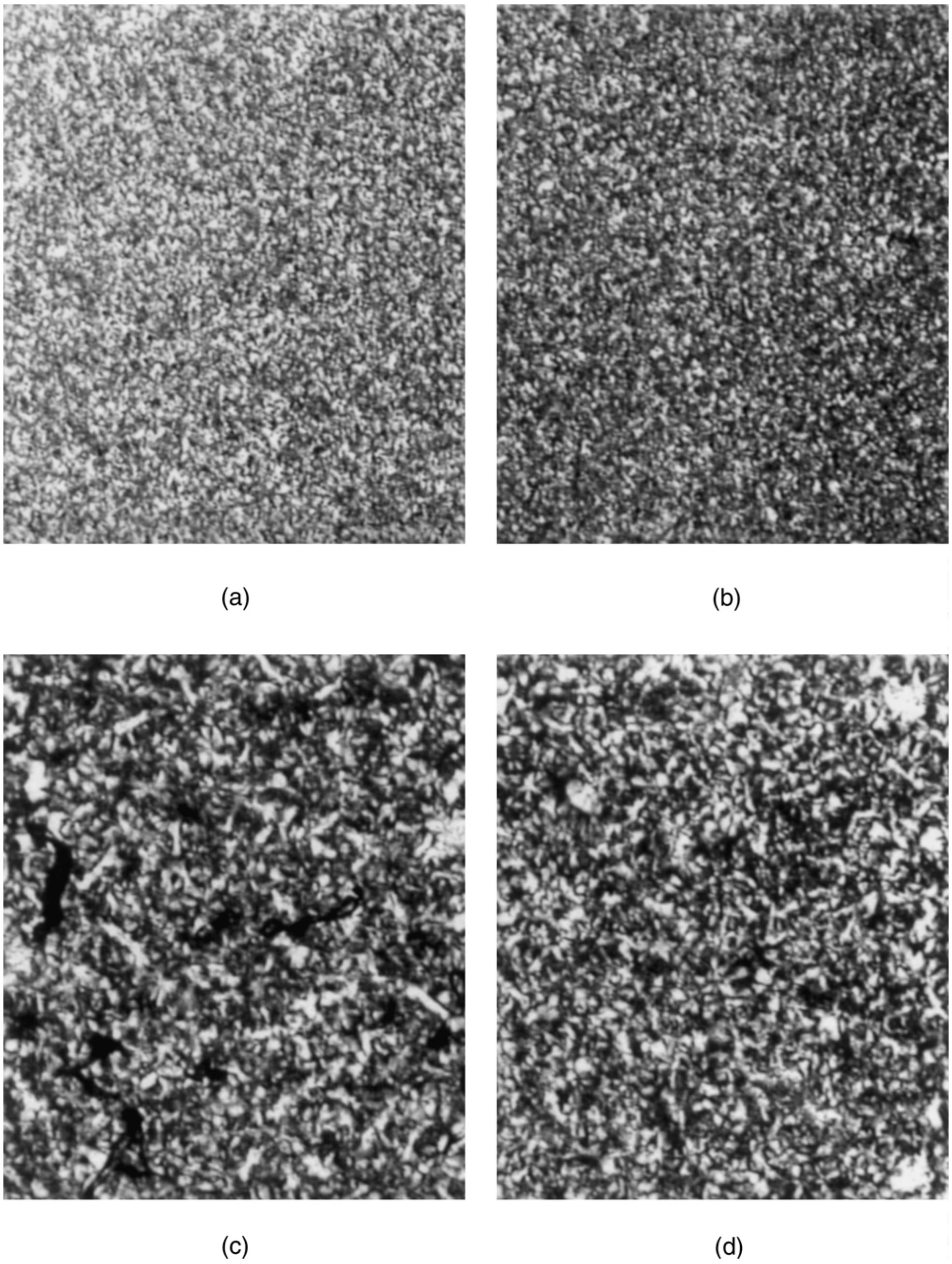

Fig. 11. Optical micrographs viewed with cross polars at 200 × magnification (i.e. 1 cm = 60 μm) of isotactic polypropylene containing (a) 0.3 wt% micron-size particles of zinc oxide (i.e. MicroZn) that were coated with 0.06 wt% OrganoCH$_3$, (b) 0.3 wt% nanoparticles of zinc oxide (i.e. NanoZn) that were coated with 0.06 wt% OrganoCH$_3$, (c) 0.3 wt% micron-size particles of zinc oxide (i.e. MicroZn) that were coated with 0.06 wt% OrganoF, and (d) 0.3 wt% nanoparticles of zinc oxide (i.e. NanoZn) that were coated with 0.06 wt% OrganoF. Samples were extruded at 239 °C from a twinscrew micro-mixer, and all photos were obtained at 120 °C.

than they are when the inorganic particles are absent in Fig. 7(a). In contrast, isotactic polypropylene exhibits a distorted spherulitic pattern in the presence of OrganoF-coated particles of MicroZn [i.e. Fig. 11(c)] or NanoZn [i.e. Fig. 11(d)]. The spherulites in Fig. 11(c) and (d) exhibit more resemblance to those in Fig. 3(b) and (c) when iPP crystallizes in the presence of MicroZn and NanoZn without OrganoF, relative to the spherulitic pattern in Fig. 7(b) when iPP crystallizes in the presence of OrganoF without zinc oxide. X-ray diffractograms (c) and (d) in Figs. 8 and 9 reveal that organic coatings on zinc oxide micro- and nanoparticles do not perturb the monoclinic crystal lattice of isotactic polypropylene, but OrganoCH_3 induces crystallization of a larger fraction of the hexagonal β-form than OrganoF.

4. Conclusions

There are only 10–15 investigations in the research literature that focus on nanoscale-size nucleating agents for polymers, in general, and even fewer that employ nanoparticles of zinc oxide. This contribution describes how zinc oxide nanoparticles coated with organic nucleating agents affect the morphology and crystallization temperature of isotactic polypropylene (i.e. iPP). Individual nanoscale-size particles of zinc oxide are approximately 40 nm, whereas agglomerated nanoparticles are 150 nm in length. The crystal structure of the α-form of isotactic polypropylene is unaffected by zinc oxide. However, X-ray diffractograms indicate that the fraction of the β-form of iPP increases in the presence of 1,3,5-benzene tricarboxylic-(*N*-2-methylcyclohexyl)triamine (i.e. OrganoCH_3). The largest spherulites are observed for pure iPP. Much smaller spherulitic textures appear in iPP samples that contain micron-size and nanoscale-size particles of zinc oxide. Nanoparticles of zinc oxide produce the smallest iPP spherulites. OrganoCH_3 is an effective nucleating agent for iPP, whereas micron-size (i.e. MicroZn) or nanoscale-size (i.e. NanoZn) particles of zinc oxide, as well as the fluorinated aromatic compound (i.e. OrganoF) do not increase the crystallization temperature of this industrially important polyolefin, beyond experimental uncertainty. OrganoCH_3 induces crystallization of iPP without the formation of spherulites. These non-spherulitic textures are also birefringent when OrganoCH_3 is coated onto either MicroZn or NanoZn. In contrast, crystallization of isotactic polypropylene in the presence of OrganoF yields fairly well-defined spherulitic patterns in the absence of zinc oxide and when this fluorinated aromatic compound is coated onto MicroZn or NanoZn. OrganoCH_3 has the highest efficiency of all four additives investigated in this study, because the crystallization temperature of iPP increases from 111 to 118 °C. Relative to isotactic polypropylene and 0.06 wt% OrganoCH_3 with $T_C = 118$ °C, OrganoCH_3-coated particles of NanoZn increase the crystallization temperature of iPP by an additional 7 °C, whereas no further enhancement in T_C occurs when OrganoCH_3 is coated onto micron-size particles of zinc oxide. Enhancements in T_C are attributed to (i) the effectiveness of OrganoCH_3 as a nucleating agent for iPP, (ii) the increase in specific surface area provided by zinc oxide nanoparticles, and (iii) efficient distribution of OrganoCH_3 via zinc oxide. This study demonstrates that the nonisothermal crystallization temperature of isotactic polypropylene increases by an additional 7 °C when an aliphatic triamine (i.e. OrganoCH_3) is efficiently distributed within the polymeric matrix by coating this nucleating agent onto zinc oxide nanoparticles.

Acknowledgements

The research described herein was supported by the Polymers Program of the National Science Foundation via Grant #DMN-0320980, the National Scientific Foundation of the Peoples Republic of China (No. 50083001) and by a grant from the Qingdao Science and Technology Committee.

References

[1] Marco C, Ellis G, Gomez MA. J Appl Polym Sci 2002;84(13): 2440–50.
[2] Chan CM, Wu JS, Li JX. Polymer 2002;43(10):2981–92.
[3] Taubert A, Glasser G, Palms D. Langmuir 2002;18(11):4488–94.
[4] Privalko VP, Karaman VM, Privalko EG, Walter R, Friedrich K, Zhang MQ, Rong MZ. J Macromol Sci—Phys 2002;B41(3):487–505.
[5] Zhang ML, Liu YQ, Zhang XH, Gao JM, Huang F, Song ZH, Wei GS, Qiao JL. Polymer 2002;43(19):5133–8.
[6] Gui QD, Xin Z, Zhu WP, Dai G. J Appl Polym Sci 2003;88(2): 297–301.
[7] Chung SC, Hahm WG, Im SS, Oh SG. Macromol Res 2002;10(4): 221–9.
[8] Ferrage E, Martin F, Boudet A. J Mater Sci 2002;37(8):1561–73.
[9] Zweifel H. Plastics additives handbook, 5th ed. Munich: Hanser; 2001. p 963–4.
[10] Wittmann JC, Lotz B. Prog Polym Sci 1990;15(6):909–48.
[11] Chisholm BJ, Fong PM, Zimmer JG, Hendrix R. J Appl Polym Sci 1999;74(4):889–99.
[12] Mercier JP. Polym Engng Sci 1990;30(5):270–8.
[13] Monks R. Plast Technol 1989;35:65.
[14] Jang GS, Cho WJ, Ha CS. J Polym Sci; Polym Phys Ed 2001;39(10): 1001–16.
[15] Song SS, White JL, Cakmak M. Polym Engng Sci 1990;30(16): 944–9.
[16] Zhang LD, Mu JM. Science of nanomaterials. Shenyang: Science and Technology Press; 1994. p 1–25.
[17] Shepard TA, Delsorbo CR, Louth RM, Walborn JL, Norman DA, Harvey NG, Spontak RJ. J Polym Sci; Polym Phys Ed 1997;35(16): 2617–28.
[18] Feng Y, Jin X, Hay JN. J Appl Polym Sci 1998;69(10):2089–95.
[19] Nagarajan K, Levon K, Myerson AS. J Therm Anal Calorimetry 2000; 59(1-2):497–508.
[20] Mercurio DJ, Spontak RJ. J Phys Chem B 2001;105(11):2091–8.
[21] Nagarajan K, Myerson AS. Cryst Growth Des 2001;1(2):131–42.

[22] Marco C, Gomez MA, Ellis G, Arribas JM. J Appl Polym Sci 2002; 84(9):1669–79.

[23] Busse K, Kressler J, Maier RD, Scherble J. Macromolecules 2000;33: 8775–80.

[24] Varga J, Mudra I, Ehrenstein GW. J Appl Polym Sci 1999;74: 2357–68.

[25] Marcincin A, Ujhelyiova A, Marcincin K, Alexy P. J Therm Anal 1996;46(2):581–95.

[26] Wu W, Xu ZD. Acta Polymerica Sinica 2000;1:99–104.

[27] Dobreva A, Gutzow I. J Non-Cryst Solids 1993;162:1–12.

[28] Dobreva A, Gutzow I. J Non-Cryst Solids 1993;162:13–25.

[29] Jang GS, Cho WJ, Ha CS, Kim W, Kim HK. Colloid Polym Sci 2002; 280(5):424–31.

[30] Wang K, Mai K, Han Z, Zeng H. J Appl Polym Sci 2001;81:78–84.

[31] Lorenzo MLD, Cimmino S, Silvestre C. J Appl Polym Sci 2001;82: 358–67.

[32] Mathieu C, Thierry A, Wittmann JC, Lotz B. J Polym Sci, Polym Phys Ed 2002;40(22):2504–15.

[33] Khoury F. J Res Nat Bureau Stand, Phys Chem A 1966;70(1):29–61.

[34] Norton DR, Keller A. Polymer 1985;26(4):704–16.

[35] Lotz B, Wittmann JC. J Polym Sci, Polym Phys Ed 1986;24(7): 1541–58.

[36] Olley RH, Bassett DC. Polymer 1989;30(3):399–409.

[37] Joint Committee on Powder Diffraction, Inorganic Index, Sarthome, PA; 1981.